Biochemical and Biophysical Research Communications 456 (2015) 768–773

Contents lists available at ScienceDirect

Biochemical and Biophysical Research Communications

journal homepage: www.elsevier.com/locate/ybbrc

# Effective internalization of U251-MG-secreted exosomes into cancer cells and characterization of their lipid components

Yuki Toda [a], Kazuyuki Takata [b], Yuko Nakagawa [a], Hikaru Kawakami [b], Shusuke Fujioka [b], Kazuya Kobayashi [a], Yasunao Hattori [a], Yoshihisa Kitamura [b], Kenichi Akaji [a], Eishi Ashihara [b,*]

[a] Department of Medicinal Chemistry, Misasagi-Shichono-cho 1, Yamashina-ku, Kyoto-shi, Kyoto 607-8412, Japan
[b] Department of Clinical and Translational Physiology, Kyoto Pharmaceutical University, Misasagi-Nakauchi-cho 5, Yamashina-ku, Kyoto-shi, Kyoto 607-8414, Japan

ARTICLE INFO

*Article history:*
Received 26 November 2014
Available online 11 December 2014

*Keywords:*
Cancer cell targeting
Drug delivery system
Exosomes
Glioblastoma
Lipid

ABSTRACT

Exosomes, the natural vehicles of various biological molecules, have been examined in several research fields including drug delivery. Although understanding of the biological functions of exosomes has increased, how exosomes are transported between cells remains unclear. We hypothesized that cell tropism is important for effective exosomal intercellular communication and that parental cells regulate exosome movement by modulating constituent exosomal molecules. Herein, we demonstrated the strong translocation of glioblastoma-derived exosomes ($U251_{exo}$) into their parental (U251) cells, breast cancer (MDA-MB-231) cells, and fibrosarcoma (HT-1080). Furthermore, disruption of proteins of $U251_{exo}$ by enzymatic treatment did not affect their uptake. Therefore, we focused on lipid molecules of $U251_{exo}$ with the expectation that they are crucial for effective incorporation of $U251_{exo}$ by cancer cells. Phosphatidylethanolamine was identified as a unique lipid component of U251-MG cell-derived extracellular vesicles. From these results, valuable insight is provided into the targeting of $U251_{exo}$ to cancer cells, which will help to develop a cancer-targeted drug delivery system.



## 1. Introduction

Systemic anti-cancer drugs often have adverse side effects; therefore, the development of drug targeting technology is important to provide safer cancer therapies [1]. Polyethylene glycol-modified nanocarrier-complexed drugs, which accumulate in tumor tissues through passive targeting, are in use. However, the desired effects, which are dependent on leaky tumor-angiogenic vessels, are not attained in all tumors because the degree of tumor vascularization can vary according to the tumor type and status [2]. The attachment of targeting moieties, such as antibodies [3], fragment antigen-binding [4], and small peptides [5], is useful for selective drug delivery by recognition of cancer-associated molecules; however, this has not had a clinical impact on human health [6].

Exosomes are extracellular vesicles (EVs) with a diameter of 50–100 nm that transport a broad array of biologically active materials, such as mRNA, microRNA, and protein, between cells [7]. These cargoes contribute to various pathological processes [8–11]. Although cancer cell-derived exosomes apparently have multiple functions in tumor progression, the detailed mechanism underlying their translocation is not understood.

Once the biological significance of exosomes have advantages for use as a drug delivery system (DDS); exosomes, which stably transport cargoes, can be used to deliver nucleic acid drugs, and the intrinsic therapeutic activity of exosomes can enhance the pharmacological effects of exosome-based drugs [12]. Exosome-mediated tumor-selective drug delivery makes exosomes an attractive DDS candidate. Exosomes can be targeted by modifying their surface ligands [13,14]. However, there is no report clearly indicating the targeting of intact exosomes to cancer cells.

In this study, we investigated whether cancer cell-derived exosomes are similarly incorporated by cancer and non-cancer cells. In addition, factors underlying efficient incorporation of glioblastoma (GBM) cell-derived exosomes by cancer cells were explored.

*Abbreviations:* AFM, atomic force microscopy; Ast, astrocyte; $Ast_{exo}$, astrocyte-derived exosomes; $Ast_{EV}$, astrocyte-derived extracellular vesicles; DIC, differential interference contrast; DLS, dynamic light scattering; EV, extracellular vesicle; GBM, glioblastoma; MDA, MDA-MB-231; PE, phosphatidylethanolamine; SM, sphingomyelin; TLC, thin-layer chromatography; $U251_{EV}$, U251-MG cell-derived extracellular vesicles; U251, U251-MG; $U251_{exo}$, U251-MG cell-derived exosomes.

* Corresponding author.
*E-mail address:* ash@mb.kyoto-phu.ac.jp (E. Ashihara).

http://dx.doi.org/10.1016/j.bbrc.2014.12.015
0006-291X/

## 2. Materials and methods

### 2.1. Cell culture

Human GBM cells (U251-MG; U251), human breast cancer cells (MDA-MB-231; MDA), and human fibrosarcoma cells (HT-1080) were obtained from the American Type Culture Collection (Manassas, VA, USA). Human astrocytes were purchased from DS Pharma Biomedical (Osaka, Japan). U251 cells, MDA cells, and astrocytes were cultured in DMEM. HT-1080 cells were cultured in EMEM containing 1% sodium pyruvate and 1% non-essential amino acids at 37 °C in 5% $CO_2$. All media were supplemented with 10% fetal calf serum, which had been depleted of EVs by ultracentrifugation at 100,000*g* for 70 min [15].

### 2.2. Exosome isolation

Exosomes were prepared from the conditioned medium of U251 cells and astrocytes as described previously [16]. Briefly, the conditioned medium of cells was centrifuged at 2,000*g* for 20 min and then at 10,000*g* for 30 min to remove dead cells and debris. EVs, including exosomes, were pelleted by ultracentrifugation at 100,000*g*. For further purification, a sucrose gradient (0.25–2.5 M sucrose) was prepared over the pellet and centrifuged at 100,000*g* for 5 h. Ten fractions were collected from the bottom of the gradient, diluted with 20 mM HEPES, and pelleted by centrifugation at 100,000*g* for 5 h. The resulting pellets containing exosomes derived from U251 cells or astrocytes ($U251_{exo}$ and $Ast_{exo}$, respectively) were used for further analyses.

### 2.3. Immunoblot analysis

Total proteins were separated by SDS–PAGE and transferred to PVDF membranes. Membranes were incubated with a primary antibody followed by a HRP-linked secondary antibody (GE Healthcare, Uppsala, Sweden). Rabbit anti-CD63 (Santa Cruz Biotechnology, Santa Cruz, CA, USA) and mouse anti-TSG101 (Abcam, Cambridge, MA, USA) antibodies were used. Protein bands were detected using enhanced chemiluminescence (GE Healthcare). To detect biotinylated proteins, HRP-streptavidin (TREVIGEN, Gaithersburg, MD, USA) was used.

### 2.4. Exosomal size distribution and imaging

The size distribution of exosomes was determined by dynamic light scattering (DLS) at 4 °C using a Zetasizer Nano instrument (Malvern Instruments, Malvern, WR, UK). The EV mixture and each fraction of the sucrose gradient were imaged using a confocal microscope (LSM 510 META, Carl Zeiss, Jena, Germany). Each sample was attached to a poly-D-lysine-coated dish (MatTek Corporation, Ashland, MA, USA). After fixation, vesicles were stained with PKH26 or PKH67 (Sigma–Aldrich, St. Louis, MO, USA). The nanostructure of exosomes was analyzed by atomic force microscopy (AFM) using previously described methods [17].

### 2.5. Enzymatic digestion of the extracellular domains of exosomal proteins

Exosomes were incubated with 0.25% trypsin at 37 °C for 5 min or with 100 μg/ml proteinase K (Merck, Darmstadt, Germany) at 37 °C for 30 min, and digestions were stopped by the addition of a protease inhibitor cocktail (Sigma–Aldrich) or 4-(2-aminoethyl) benzenesulfonyl fluoride hydrochloride (Wako, Osaka, Japan), respectively. Digested exosomes were pelleted by ultracentrifugation at 100,000*g* for 70 min. Alternatively, the surface proteins of exosomes were biotinylated with NHS-biotin (Sigma–Aldrich), and biotinylated proteins were purified using a streptavidin-immobilised column (GE Healthcare).

### 2.6. Cellular internalization analysis

Exosomes were labeled with the green fluorescent dye PKH67 as described previously [9]. U251 cells and astrocytes were cultured for 9 h, after which the medium was replaced with that containing PKH-labeled exosomes. After incubation at 37 °C for 12 h, cells were gently washed with PBS, fixed, and incubated with Rhodamine-phalloidin conjugate and Hoechst 33,258 (both from Life Technologies, Carlsbad, CA, USA) to visualize the actin cytoskeleton and nuclei, respectively. A laser scanning confocal microscope was used to detect fluorescence and to collect differential interference contrast (DIC) images. For semi-quantitative analysis, images of red fluorescence (actin cytoskeleton) and green fluorescence (intracellular exosomes) were used (WinRoof; MITANI CORPORATION, Fukui, Japan). Based on the DIC images, green fluorescence intensity per cell area was calculated. Alternatively, cells were incubated with exosomes for 12 h, trypsinized, and collected. The fluorescence intensity of PKH67 per cell was determined using a flow cytometer (FACS Caliber, BD Bioscience, Franklin Lakes, NJ, USA).

### 2.7. Plasma membrane isolation

Cells were disrupted using a Dounce homogenizer in hypotonic conditions and aliquots of the homogenate were sequentially centrifuged (1000*g* for 7 min, 2000*g* for 30 min, 5000*g* for 30 min, and 12,000*g* for 70 min). The 12,000*g* pellet, which contained plasma membranes but not nuclei or mitochondria (confirmed by immunoblotting), was used in lipid analysis.

### 2.8. Lipid extraction and thin-layer chromatography (TLC)

The standard sample was a mixture of each class of lipids obtained from Avanti Polar Lipids (Alabaster, AL, USA): 1-stearoyl-2-arachidonoyl-*sn*-glycero-3-phosphocholine, 1-stearoyl-2-arachidonoyl-*sn*-glycero-3-phosphoethanolamine, liver phosphatidylinositol, 1-palmitoyl-2-oleoyl-*sn*-glycero-3-phospho-L-serine, N-stearoyl-D-*erythro*-sphingosylphosphorylcholine, and cholesterol. Total lipids of EVs and plasma membranes were extracted using the Bligh and Dyer method [18]. Each phospholipid class was separated by TLC on silica plates (Merck, Darmstadt, Germany) following the method of Yao and Rastetter [19].

### 2.9. Statistical evaluation

Results of confocal microscopy and TLC analyses are given as the mean ± standard error of the mean. Means were compared using the two-tailed unpaired Student's *t* test or a one-way ANOVA with the Bonferroni/Dunn test (Prism, GraphPad Software, San Diego, CA, USA). $P < 0.05$ was considered significant.

## 3. Results

### 3.1. Preparation of ultrapure exosomes by ultracentrifugation and density gradient separation

The conditioned medium of U251 cells was sequentially centrifuged at increasing centrifugal force, eventually generating a 100,000*g* pellet. In western blot analysis, the exosomal markers CD63 and TSG101 were detected in this pellet (Fig. 1A). However, particles of various sizes were detected by confocal microscopy

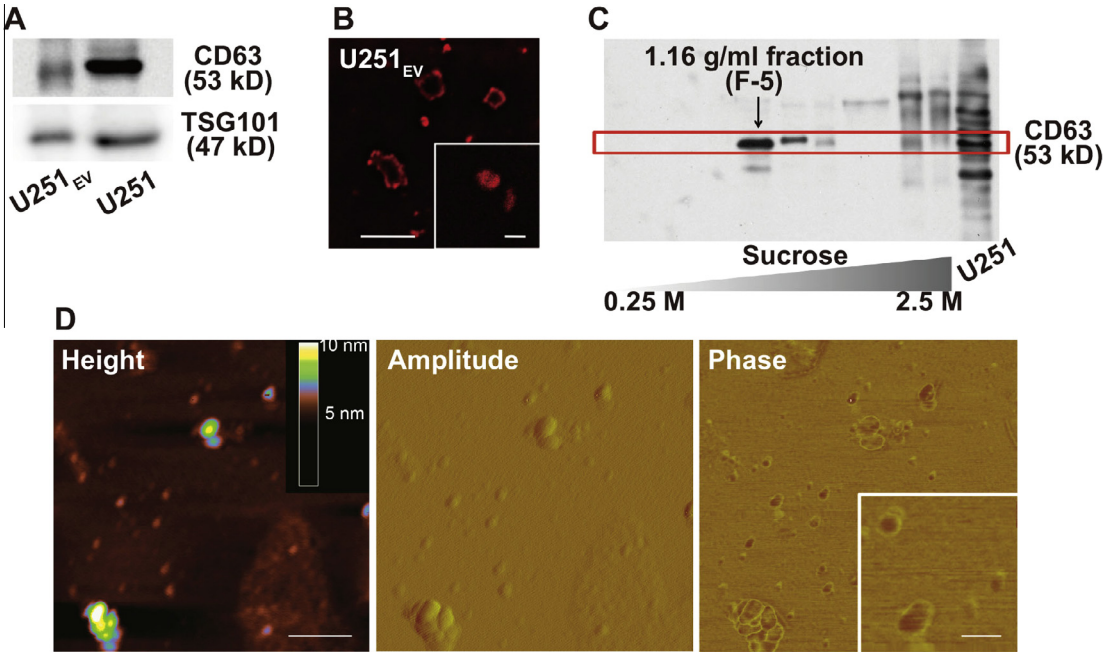


**Fig. 1.** Purification of U251-MG cell-derived exosomes by ultracentrifugation and density gradient separation. (A) The 100,000*g* pellets ($U251_{EV}$) were analyzed for the exosome-enriched proteins CD63 and TSG101. (B) Isolated $U251_{EV}$ were labeled with PKH and examined by laser scanning confocal microscopy (bar, 2 μm). Inset: an exosome-sized particle (bar, 100 nm). (C) The 100,000*g* pellets were subjected to density gradient separation and the resulting fractions were labeled with an anti-CD63 antibody. (D) Particles in 1.16 g/ml fraction (F-5) were imaged by atomic force microscopy (AFM) (bar, 400 nm). AFM topographic (left), amplitude (middle), and phase (right) images of $U251_{exo}$. Inset: $U251_{exo}$ with a core region of a reduced density (bar, 100 nm).

analysis of this pellet (Fig. 1B), suggesting that further purification using a sucrose gradient was required. Following density gradient separation of the 100,000*g* pellet, CD63 was mainly located in a 1.16 g/ml fraction (F-5); larger particles were observed in higher density fractions (Fig. 1C and Supplementary Fig. S1). These data suggest that density gradient separation was necessary to obtain a pure population of EVs. In DLS analysis, the size distribution of particles in F-5 ranged from 50 to 100 nm, which corresponds to the size of exosomes, whereas particles larger than 200 nm were rarely detected (Supplementary Fig. S2). AFM was performed to analyze the nanostructure of $U251_{exo}$. The 3D structure and vesicular organization of $U251_{exo}$ was measured at the nanometer level by acquiring topographic (height), amplitude, and phase images (which allow variations in properties such as exosome density and viscoelasticity to be mapped) using AFM tapping mode in air. This showed that $U251_{exo}$ were non-uniform in size and their morphology was circular or cup-shaped with a core region of a lower density, implying that the particles were hollow (Fig. 1D).

### 3.2. Effective internalization of $U251_{exo}$ by various cancer cells

To examine the intercellular trafficking of $U251_{exo}$, we performed confocal microscopy analysis of U251 cells and astrocytes after treatment with PKH-labeled $U251_{exo}$ for 12 h. The concentration of $U251_{exo}$ was represented as the ratio between the number of cells from which $U251_{exo}$ were derived (donor cells) and the number of treated cells. Green fluorescence in U251 cells strongly increased in a concentration-dependent manner, while it increased moderately in astrocytes (Supplementary Fig. S3A). When there were 10–50-fold more donor cells than treated cells, $U251_{exo}$ were internalized significantly more by U251 cells than by astrocytes (Fig. 2A and Supplementary Fig. S3B). By contrast, $U251_{exo}$ internalization by U251 cells and astrocytes was similar when there were 100-fold more donor cells than treated cells, meaning that uptake was saturated. In flow cytometric analysis, the histogram of PKH fluorescence intensity in U251 cells was shifted to the right of that in astrocytes (Fig. 2B and Supplementary Fig. S3C). Moreover, MDA cells significantly incorporated $U251_{exo}$ (Fig. 2C and D). HT-1080 cells also internalized $U251_{exo}$ (not significant). These findings showed that $U251_{exo}$ were taken up more effectively by some cancer cells than by astrocytes.

Additionally, we investigated whether $Ast_{exo}$ were effectively taken up by U251 cells. To compare the internalization efficiency of $U251_{exo}$ and $Ast_{exo}$, their protein concentration, rather than the number of donor cells, was used because exosomal secretion likely differs among cells. The incorporation of $Ast_{exo}$ into U251 cells was significantly lower than that of $U251_{exo}$ (Supplementary Fig. S4). These results suggest that U251 cells recognize $U251_{exo}$ to facilitate their effective internalization.

### 3.3. Protein ligand-independent interaction of $U251_{exo}$ with U251 cells

Various surface molecules on exosomes participate in the first step of their contact with cells. To elucidate whether protein ligands on the surface of $U251_{exo}$ are involved in their effective translocation into cancer cells, trypsin was used to remove all surface proteins from $U251_{exo}$ [20]. Biotinylated proteins migrated at a lower molecular weight following trypsin treatment, confirming that the surface proteins of exosomes were disrupted (Fig. 3A). Trypsin-treated and mock-treated $U251_{exo}$ were incorporated similarly into U251 cells (Fig. 3B and C). Moreover, uptake of $U251_{exo}$ by U251 cells was not affected by treatment with proteinase K, which has a broad substrate specificity [21] (Supplementary Fig. S5).

### 3.4. Phosphatidylethanolamine (PE) is a unique lipid component of $U251_{exo}$

Our results suggest that other factors, aside from surface protein ligands, are involved in the effective incorporation of

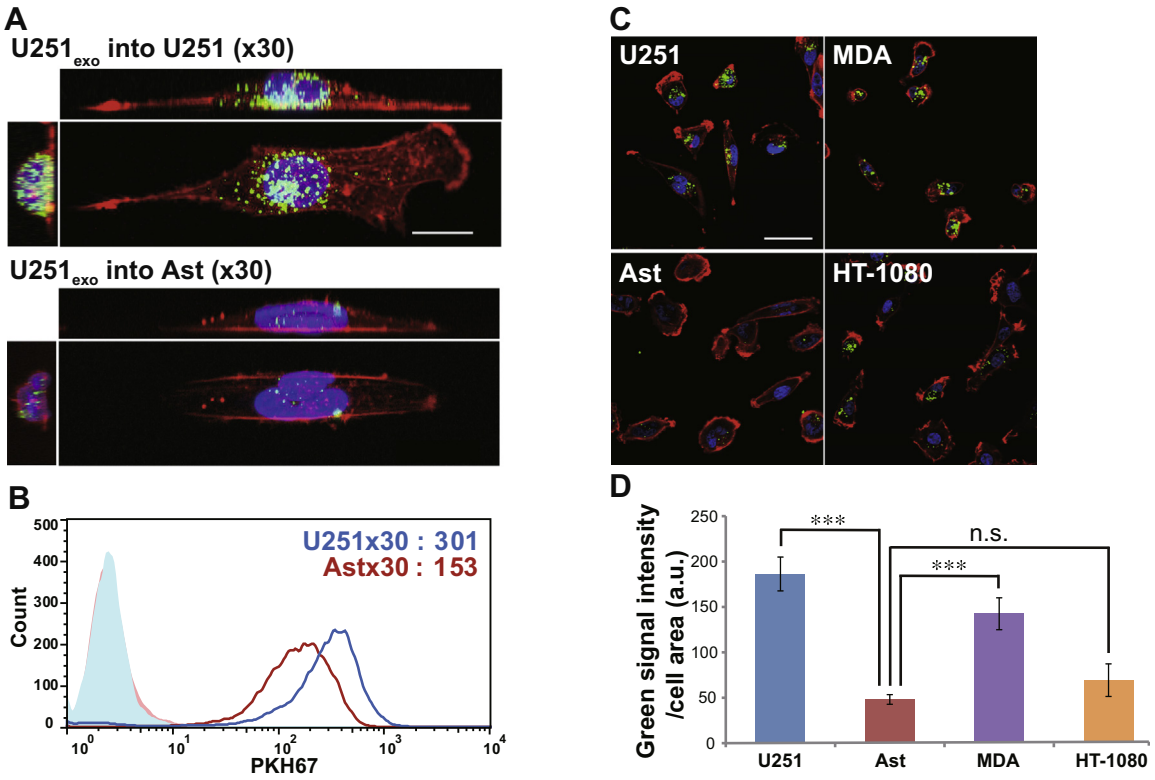


**Fig. 2.** Effective uptake of U251-MG (U251) cell-derived exosomes ($U251_{exo}$) by their parental cells and by other cancer cell lines. (A) Reconstructed 3D images of $U251_{exo}$ in U251 cells and Ast, when there were 30-fold more donor cells than treated cells (bar, 20 μm). $U251_{exo}$ were labeled with PKH67 and added to U251 cells or astrocytes (Ast). After 12 h, cells were fixed and stained with Rhodamine-phalloidin conjugate and Hoechst 33,258, and imaged by laser scanning confocal microscopy. (B) Fluorescence of U251 cells and Ast following treatment with $U251_{exo}$ was evaluated by flow cytometry. Numbers show the median fluorescence intensity. (C) U251 cells, MDA-MB-231 (MDA) cells, HT-1080 cells, and Ast were treated with $U251_{exo}$ for 12 h (bar, 50 μm). (D) Green fluorescence intensity per cell area was determined by image analysis ($n = 30$ cells per group). Bars indicate the mean ± SEM. $^{***}P < 0.001$. n.s.: not significant. a.u.: arbitrary unit.

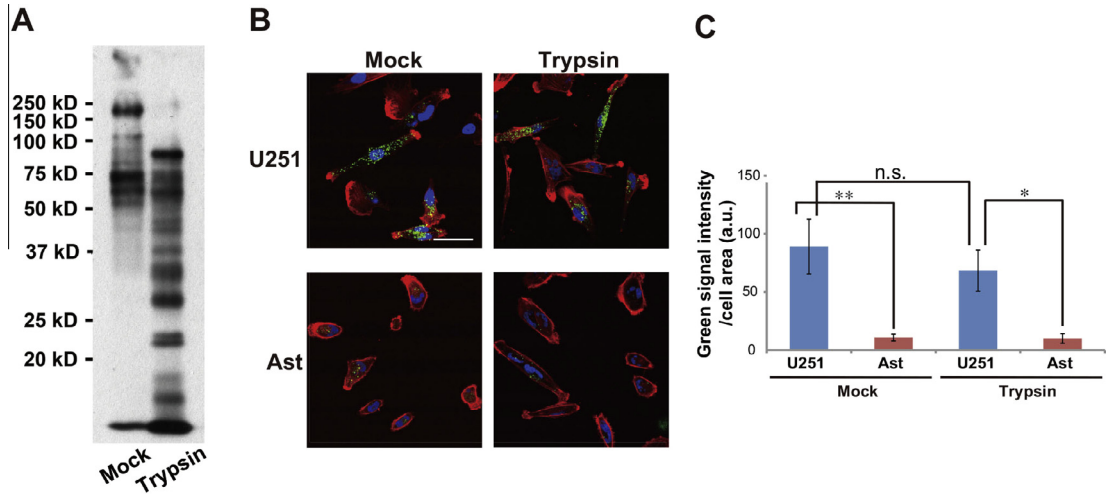


**Fig. 3.** Ligand–receptor interactions are not involved in the uptake of U251-MG (U251) cell-derived exosomes ($U251_{exo}$) by U251 cells. (A) Protein ligands on the surface of $U251_{exo}$ were digested by treatment with trypsin at 37 °C for 5 min. Cleaved proteins on the membrane were labeled with NHS-biotin and analyzed by immunoblotting with HRP-streptavidin. (B) Mock-treated and trypsin-treated $U251_{exo}$ were labeled with PKH67 and incubated with U251 cells and astrocytes (Ast) for 12 h (bar, 50 μm). (C) Green fluorescence intensity per cell area was determined by image analysis ($n = 30$ cells per group). Bars indicate the mean ± standard error of the mean. $^{*}P < 0.05$, $^{**}P < 0.01$. n.s.: not significant. a.u.: arbitrary unit.

$U251_{exo}$ into cancer cells. Therefore, we focused on the lipid components of $U251_{exo}$. Lipid components vary among exosomes according to their parental cells and among the plasma membranes of different cells [22]. Our attempts to assess the lipid compositions of $U251_{exo}$ and $Ast_{exo}$ by TLC were not successful because their lipid concentrations were too low to be detected. Instead, we compared the lipid compositions of EVs derived from U251 cells and astrocytes ($U251_{EV}$ and $Ast_{EV}$, respectively). The ratio of sphingomyelin (SM) to total lipids was significantly lower in $U251_{EV}$ than in $Ast_{EV}$ (Fig. 4). The percentage of PE was significantly

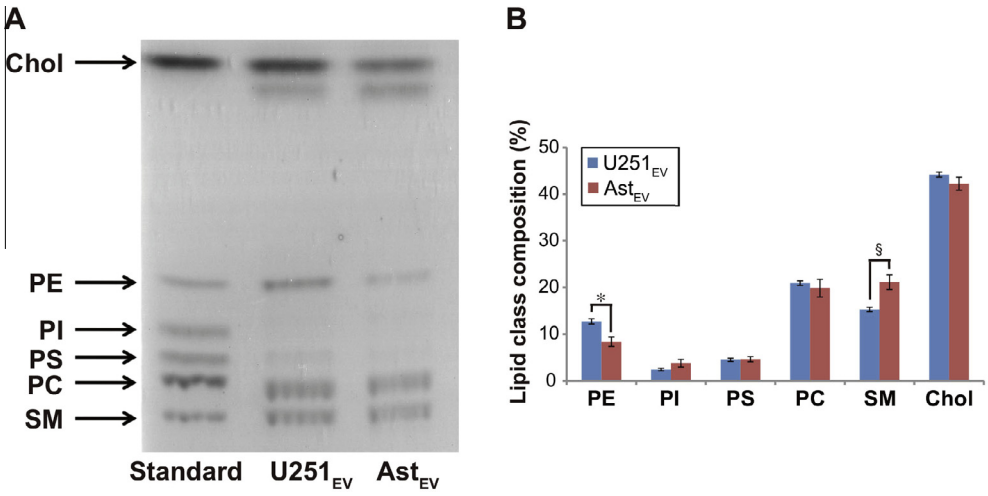


**Fig. 4.** The percentages of phosphatidylethanolamine (PE) and sphingomyelin (SM) differ between extracellular vesicles derived from U251-MG (U251) cells ($U251_{EV}$) and astrocytes ($Ast_{EV}$). (A) Lipid extracts of $U251_{EV}$ and $Ast_{EV}$ were analyzed by thin-layer chromatography. (B) The percentage of the total lipid content constituted by each lipid class was determined by image analysis ($n = 3$). Bars indicate the mean ± standard error of the mean (SEM). $^{*}P < 0.05$. PI, phosphatidylinositol; PS, phosphatidylserine; PC, phosphatidylcholine; Chol, cholesterol.

higher in $U251_{EV}$ than in $Ast_{EV}$. The plasma membrane of U251 cells included PE significantly compared with that of astrocytes (Supplementary Fig. S6). These observations suggest that the lipid components of EVs, especially PE and SM, differ according to the cells from which they are derived, and that this difference is partly owing to the lipid characteristics of the parental cell membranes.

## 4. Discussion

A major obstacle in understanding the nature of exosomes is the lack of consensus regarding the definition of an exosome, which has led to wide variation in the methods used to prepare and identify exosomes among studies [23]. Many types of EVs containing exosomes have been classified according to their origin, size, and density [24]. Although ultracentrifugation is frequently used in many exosome isolation methods [8,10], it generated a highly heterogeneous population in the current study. Further purification by density gradient separation improved this heterogeneity. The resulting sample ($U251_{exo}$) contained particles with a diameter of around 100 nm that expressed CD63 in a 1.16 g/cm$^3$ fraction.

Electron microscopy is the most commonly used technique to characterize the morphology of exosomes [7,16]; however, vesicles in fixed samples adopt an apparent 2D cup-shape under vacuum conditions that does not necessarily reflect their original morphology. Low-force AFM imaging of unstained and unfixed samples under ambient conditions appears to be far less damaging to exosomes. Moreover, AFM has a subnanometer resolution imaging capability, not far below that of transmission electron microscopy, which allows structural variation among exosomes to be studied. The morphological difference between healthy donor-derived and cancer patient-derived salivary exosomes has been described using AFM imaging in air [25]. We confirmed the existence of exosomes in F-5 by AFM analysis in ambient conditions and described the characteristics of $U251_{exo}$.

The potential use of endogenous exosomes for cell-to-cell communication has created excitement in the drug delivery field because such carriers appear to have several advantages over existing artificial DDS. We believe that a great benefit of the use of exosomes as a DDS is their ability to target specific cells. Exosomes have been targeted to specific cell types using virus-derived proteins or peptide ligands [13,14]. However, these targeting strategies are not dependent on the intrinsic nature of exosomes, but on the exogenously added protein/peptide ligands. By contrast, our concept is based on the application of naturally targeted exosomes. $U251_{exo}$ were efficiently incorporated into their parental cells and other cancer cells, making this a candidate carrier for targeted drug delivery. Whether exosomes exhibit cell tropism remains controversial. Another type of GBM (U87-MG)-derived exosomes are internalized by cells of several species [26], but the efficiency of their uptake appears to be significantly higher in parental cells than in other cells. Feng et al. reported that the efficiency with which human leukemia cell (K562 or MT-4)-derived exosomes are internalized is influenced by the phagocytic activity of recipient cells [27]. By contrast, uptake of $U251_{exo}$ and $Ast_{exo}$ by U251 cells differed, indicating that U251 cells do not take up exosomes non-specifically. $U251_{exo}$ may stimulate the endocytic activity of U251 cells. Thus, the cancer cell tropism of $U251_{exo}$ is not owing to the high endocytic activity of parental cells, but to the unique components of $U251_{exo}$.

Despite promising results suggesting that U251-derived exosomes could be used to target cancer cells, several hurdles need to be overcome prior to clinical translation. The clinical safety of exosomes is of most concern. We do not completely understand the contents or functions of exosomes, meaning that their clinical administration may have unexpected side effects. We believe that this concern could be overcome by converting multifunctional exosomes into artificial drug carriers that specifically target cancer cells.

Identifying the unique components of $U251_{exo}$ is required to mimic their cancer cell targeting. However, the molecular factors that are important for the cellular incorporation of exosomes are not completely understood and may vary according to the origin of the exosomes and recipient cells. Ligand–receptor interactions between exosomes and cells are a key element in the initial step of exosome internalization. Some adhesion molecules (CD11a and CD54) on dendritic cell-derived exosomes are involved in the incorporation of these exosomes into their parental cells [28]. In the present study, enzymatic treatment disrupted surface proteins on $U251_{exo}$ but did not affect their uptake by parental cells. These results show that proteins on exosomal membranes are not associated with exosome internalization.

In addition to proteins, lipids of exosomes are also reportedly involved in their uptake and function [15] and [20]. The unique lipids of PC3-derived exosomes contributed to cellular adherence/internalization [29]. Therefore, we hypothesized that U251

cells recognize the unique lipid components of $U251_{exo}$. In TLC analysis, the percentages of SM and PE differed between $U251_{exo}$ and $Ast_{exo}$. Enrichment of SM and monosialodihexosylganglioside in acidic-cultured melanoma-derived exosomes positively affects their ability to fuse by increasing their membrane rigidity [15]. However, this was not applicable to the uptake of $U251_{exo}$, whose SM content was lower than that of $Ast_{EV}$. PE has a cone-shaped structure and can promote a bilayer-to-hexagonal transition, which may facilitate fusion by increasing negative membrane curvature [30]. PE was abundant in the plasma membranes and exosomes of U251 cells, and this may assist the internalization of $U251_{exo}$ by these cells. A direct causal relationship between effective incorporation of $U251_{exo}$ and their lipid molecules (SM and PE) will be investigated in the future.

In conclusion, U251-derived exosomes were potently and specifically incorporated into cancer cells and were taken up by their parental cells independently of surface protein ligands on exosomes. Lipid analysis identified PE as a unique component of $U251_{EV}$. We propose that further characterization of $U251_{exo}$ will provide critical insight into cancer cell targeting and the mechanisms underlying intercellular communication via EVs.

## Acknowledgments

We thank Dr. Tohru Wakatsuki (Kyoto Pharmaceutical University) for the density gradient separation technique. This work was supported in part by a grant-in-aid for scientific research from the Ministry of Education, Culture, Sports, Science, and Technology of Japan (26·2568 to Y.T., 25460160 to K.A., and 23591404 to E.A.) and the Adaptable and Seamless Technology Transfer Program through target-driven R&D of the Japan Science and Technology Agency (231Z01044). Y.T. is grateful to Research Fellowships for Young Scientists from the Japan Society for the Promotion of Science.

## Appendix A. Supplementary data

Supplementary data associated with this article can be found, in the online version, at http://dx.doi.org/10.1016/j.bbrc.2014.12.015.

## References

[1] K.B. Sutradhar, M.L. Amin, Nanotechnology in cancer drug delivery and selective targeting, ISRN Nanotechnol. 2014 (2014) 1–12.
[2] Y.H. Bae, Drug targeting and tumor heterogeneity, J. Control. Release 133 (2009) 2–3.
[3] D. Peer, E.J. Park, Y. Morishita, C.V. Carman, M. Shimaoka, Systemic leukocyte-directed siRNA delivery revealing cyclin D1 as an anti-inflammatory target, Science 319 (2008) 627–630.
[4] W.W. Cheng, T.M. Allen, Targeted delivery of anti-CD19 liposomal doxorubicin in B-cell lymphoma: a comparison of whole monoclonal antibody, Fab' fragments and single chain Fv, J. Controlled Release 126 (2008) 50–58.
[5] S.H. Kim, J.H. Jeong, S.H. Lee, S.W. Kim, T.G. Park, LHRH receptor-mediated delivery of siRNA using polyelectrolyte complex micelles self-assembled from siRNA-PEG-LHRH conjugate and PEI, Bioconjugate Chem. 19 (2008) 2156–2162.
[6] M.K. Yu, J. Park, S. Jon, Targeting strategies for multifunctional nanoparticles in cancer imaging and therapy, Theranostics 2 (2012) 3–44.
[7] H. Valadi, K. Ekstrom, A. Bossios, M. Sjostrand, J.J. Lee, J.O. Lotvall, Exosome-mediated transfer of mRNAs and microRNAs is a novel mechanism of genetic exchange between cells, Nat. Cell Biol. 9 (2007) 654–659.
[8] H. Sheng, S. Hassanali, C. Nugent, L. Wen, E. Hamilton-Williams, P. Dias, Y.D. Dai, Insulinoma-released exosomes or microparticles are immunostimulatory and can activate autoreactive T cells spontaneously developed in nonobese diabetic mice, J. Immunol. 187 (2011) 1591–1600.
[9] K. Yuyama, H. Sun, S. Mitsutake, Y. Igarashi, Sphingolipid-modulated exosome secretion promotes clearance of amyloid-beta by microglia, J. Biol. Chem. 287 (2012) 10977–10989.
[10] R.A. Kore, E.C. Abraham, Inflammatory cytokines, interleukin-1 beta and tumor necrosis factor-alpha, upregulated in glioblastoma multiforme, raise the levels of CRYAB in exosomes secreted by U373 glioma cells, Biochem. Biophys. Res. Commun. 453 (2014) 326–331.
[11] Y. Xie, X. Zhang, T. Zhao, W. Li, J. Xiang, Natural CD8(+)25(+) regulatory T cell-secreted exosomes capable of suppressing cytotoxic T lymphocyte-mediated immunity against B16 melanoma, Biochem. Biophys. Res. Commun. 438 (2013) 152–155.
[12] S.A. Kooijmans, P. Vader, S.M. van Dommelen, W.W. van Solinge, R.M. Schiffelers, Exosome mimetics: a novel class of drug delivery systems, Int. J. Nanomed. 7 (2012) 1525–1541.
[13] L. Alvarez-Erviti, Y. Seow, H. Yin, C. Betts, S. Lakhal, M.J. Wood, Delivery of siRNA to the mouse brain by systemic injection of targeted exosomes, Nat. Biotechnol. 29 (2011) 341–345.
[14] S. Ohno, M. Takanashi, K. Sudo, S. Ueda, A. Ishikawa, N. Matsuyama, K. Fujita, T. Mizutani, T. Ohgi, T. Ochiya, N. Gotoh, M. Kuroda, Systemically injected exosomes targeted to EGFR deliver antitumor microRNA to breast cancer cells, Mol. Ther. 21 (2013) 185–191.
[15] I. Parolini, C. Federici, C. Raggi, L. Lugini, S. Palleschi, A. De Milito, C. Coscia, E. Iessi, M. Logozzi, A. Molinari, M. Colone, M. Tatti, M. Sargiacomo, S. Fais, Microenvironmental pH is a key factor for exosome traffic in tumor cells, J. Biol. Chem. 284 (2009) 34211–34222.
[16] C. Thery, S. Amigorena, G. Raposo, A. Clayton, Isolation and characterization of exosomes from cell culture supernatants and biological fluids, Curr. Protoc. Cell Biol. (2006), http://dx.doi.org/10.1002/0471143030.cb0322s30 (Chapter 3 Unit 3.22).
[17] H. Kawashima, Y. Sohma, T. Nakanishi, H. Kitamura, H. Mukai, M. Yamashita, K. Akaji, Y. Kiso, A new class of aggregation inhibitor of amyloid-beta peptide based on an O-acyl isopeptide, Bioorg. Med. Chem. 21 (2013) 6323–6327.
[18] E.G. Bligh, W.J. Dyer, A rapid method of total lipid extraction and purification, Can. J. Biochem. Physiol. 37 (1959) 911–917.
[19] J.K. Yao, G.M. Rastetter, Microanalysis of complex tissue lipids by high-performance thin-layer chromatography, Anal. Biochem. 150 (1985) 111–116.
[20] E. Ristorcelli, E. Beraud, P. Verrando, C. Villard, D. Lafitte, V. Sbarra, D. Lombardo, A. Verine, Human tumor nanoparticles induce apoptosis of pancreatic cancer cells, FASEB J. 22 (2008) 3358–3369.
[21] E. Kraus, U. Femfert, Proteinase K from the mold Tritirachium album Limber. Specificity and mode of action, Hoppe Seylers Z. Physiol. Chem. 357 (1976) 937–947.
[22] C. Subra, K. Laulagnier, B. Perret, M. Record, Exosome lipidomics unravels lipid sorting at the level of multivesicular bodies, Biochimie 89 (2007) 205–212.
[23] D.S. Choi, D.K. Kim, Y.K. Kim, Y.S. Gho, Proteomics, transcriptomics and lipidomics of exosomes and ectosomes, Proteomics 13 (2013) 1554–1571.
[24] C. Thery, M. Ostrowski, E. Segura, Membrane vesicles as conveyors of immune responses, Nat. Rev. Immunol. 9 (2009) 581–593.
[25] S. Sharma, B.M. Gillespie, V. Palanisamy, J.K. Gimzewski, Quantitative nanostructural and single-molecule force spectroscopy biomolecular analysis of human-saliva-derived exosomes, Langmuir 27 (2011) 14394–14400.
[26] K.J. Svensson, H.C. Christianson, A. Wittrup, E. Bourseau-Guilmain, E. Lindqvist, L.M. Svensson, M. Morgelin, M. Belting, Exosome uptake depends on ERK1/2-heat shock protein 27 signaling and lipid Raft-mediated endocytosis negatively regulated by caveolin-1, J. Biol. Chem. 288 (2013) 17713–17724.
[27] D. Feng, W.L. Zhao, Y.Y. Ye, X.C. Bai, R.Q. Liu, L.F. Chang, Q. Zhou, S.F. Sui, Cellular internalization of exosomes occurs through phagocytosis, Traffic 11 (2010) 675–687.
[28] A.E. Morelli, A.T. Larregina, W.J. Shufesky, M.L. Sullivan, D.B. Stolz, G.D. Papworth, A.F. Zahorchak, A.J. Logar, Z. Wang, S.C. Watkins, L.D. Falo Jr., A.W. Thomson, Endocytosis, intracellular sorting, and processing of exosomes by dendritic cells, Blood 104 (2004) 3257–3266.
[29] T.J. Smyth, J.S. Redzic, M.W. Graner, T.J. Anchordoquy, Examination of the specificity of tumor cell derived exosomes with tumor cells in vitro, Biochim. Biophys. Acta 2014 (1838) 2954–2965.
[30] L.V. Chernomordik, M.M. Kozlov, Membrane hemifusion: crossing a chasm in two leaps, Cell 123 (2005) 375–382.